Theor Chem Acc (1998) 99:44–52

Theoretical
Chemistry Accounts

Regular article

Second-order quantum similarity measures from intracule and extracule densities

Xavier Fradera, Miquel Duran, Jordi Mestres*

Department of Chemistry and Institute for Computational Chemistry, University of Girona, E-17071 Girona, Catalonia, Spain

Received: 7 July 1997 / Accepted: 29 October 1997

Abstract. The calculation of quantum similarity measures from second-order density functions contracted to intracule and extracule densities obtained at the Hartree-Fock level is presented and applied to a series of atoms, (He, Li, Be, and Ne), isoelectronic molecules (C_2H_2, HCN, CNH, CO, and N_2), and model hydrogen-transfer processes (H_2/H^+, $H_2/H^{\bullet}$, H_2/H^-). Second-order quantum similarity measures and indices are found to be suitable measures for quantitatively analyzing electron-pair density reorganizations in atoms, molecules, and chemical processes. For the molecular series, a comparative analysis between the topology of pairwise similarity functions as computed from one-electron, intracule, and extracule densities is carried out and the assignment of each particular local similarity maximum to a molecular alignment discussed. In the comparative study of the three hydrogen-transfer reactions considered, second-order quantum similarity indices are found to be more sensitive than first-order indices for analyzing the electron-density reorganization between the reactant complex and the transition state, thus providing additional insights for a better understanding of the mechanistic aspects of each process.

Key words: Quantum similarity – Similarity measures and indices – One-electron density – Intracule and extracule densities – Molecular alignment

1 Introduction

Since the original definition of a quantum similarity measure [1] between two quantum objects, A and B, as the overlap integral of the corresponding first-order density functions, $\rho_A(\mathbf{r})$ and $\rho_B(\mathbf{r})$,

$$Z_{AB} = \int \rho_A(\mathbf{r})\rho_B(\mathbf{r})\, d\mathbf{r} \quad . \tag{1}$$

an increasing number of studies in this field have provided evidence for the applicability of quantum similarity measures as a useful tool for quantitatively analyzing electron-density redistributions in a wide range of chemical problems [2–9]. In particular, they have been employed for studying the electron-density reorganization suffered by atoms in molecules [2], molecular fragments or groups in series of molecules [3, 4], an isoelectronic series of molecules [5], and molecular complexes along a reaction coordinate [6]. They have also been used to examine the effect of a uniform electric field [6], solvation [7], torsional rotations [8], and different levels of theory [9]. However, comparisons between the electronic characteristics of atoms and molecules have so far mainly been restricted to one-electron density distributions.

One step further would imply exploring how similar the electron-pair characteristics of two quantum objects are when represented by their second-order density functions, $\Gamma_A(\mathbf{r}_1,\mathbf{r}_2)$ and $\Gamma_B(\mathbf{r}_1,\mathbf{r}_2)$. On this basis, the definition of a second-order quantum similarity measure is straightforward [10],

$$Z_{AB}^{(2)} = \int \Gamma_A(\mathbf{r}_1,\mathbf{r}_2)\Gamma_B(\mathbf{r}_1,\mathbf{r}_2)\, d\mathbf{r}_1\, d\mathbf{r}_2 \quad , \tag{2}$$

as a natural extension of the first-order quantum similarity measure given by Eq. (1). In this sense, efforts have been made to simplify the evaluation of $Z_{AB}^{(2)}$ in Eq. (2) through the use of geminal expansions of electron-pair densities within a semiempirical framework [11, 12].

Since an electron-pair density, $\Gamma(\mathbf{r}_1,\mathbf{r}_2)$, is a function of six variables and hence difficult to study in detail, the use of intracule, $\mathbf{r} = \mathbf{r}_1 - \mathbf{r}_2$, and extracule, $\mathbf{R} = (\mathbf{r}_1 + \mathbf{r}_2)/2$, coordinates [13] to reduce its dimensionality has recently received significant attention [14–21]. Accordingly, intracule, $I(\mathbf{r})$, and extracule, $E(\mathbf{R})$, densities can be defined from the corresponding coordinates as

$$I(\mathbf{r}) = \int \Gamma(\mathbf{r}_1,\mathbf{r}_2)\delta((\mathbf{r}_1 - \mathbf{r}_2) - \mathbf{r})\, d\mathbf{r}_1\, d\mathbf{r}_2 \quad , \tag{3}$$

Present address: Computational Medicinal Chemistry, N.V. Organon, 5340 BH Oss, The Netherlands

Correspondence to: J. Mestres

$$E(\mathbf{R}) = \int \Gamma(\mathbf{r}_1, \mathbf{r}_2)\delta((\mathbf{r}_1 - \mathbf{r}_2) + \mathbf{r})/2 - \mathbf{R})\, d\mathbf{r}_1\, d\mathbf{r}_2 \ . \quad (4)$$

$I(\mathbf{r})$ and $E(\mathbf{R})$ are the probability density functions for the interparticle distance and for the center of mass of an electron pair, respectively, and have the advantage of retaining some of the original two-electron character [22]. $I(\mathbf{r})$ has the particular property of being invariant to translations of the molecule and shows a center of inversion at the origin. In contrast, $E(\mathbf{R})$ retains the spatial arrangement of the nuclear framework and its origin depends upon the molecular coordinates. Both $I(\mathbf{r})$ and $E(\mathbf{R})$ are normalized to the number of electron pairs.

The recent description of a more efficient algorithm to compute $I(\mathbf{r})$ and $E(\mathbf{R})$ on large grids of points [19] has allowed analysis of their topology [20] and their respective Laplacians [21] to be extended to larger molecules. Therefore, it also provides a feasible means of numerically evaluating second-order quantum similarity measures from intracule, Y_{AB}, and extracule, X_{AB}, densities

$$Y_{AB} = \int I_A(\mathbf{r}) I_B(\mathbf{r}) d\mathbf{r} \ , \quad (5)$$

$$X_{AB} = \int E_A(\mathbf{R}) E_B(\mathbf{R}) d\mathbf{R} \ . \quad (6)$$

The aims of the present study are to scrutinize, first, the presence of similar trends between Z_{AA}, Y_{AA} and X_{AA} similarity functions when superimposing two molecules and, second, the use of second-order quantum similarity measures and indices for quantitatively analyzing electron-pair density reorganizations in series of atoms, molecules, and chemical reactions. A brief description of some computational aspects is presented in the next section, followed by a discussion of the results obtained for a series of atoms, (He, Li, Be, and Ne), isoelectronic molecules (C_2H_2, HCN, CNH, CO, and N_2), and model hydrogen-transfer reactions (H_2/H^+, $H_2/H^\bullet$, H_2/H^-).

2 Computational details

As a first approximation, all calculations in this work were performed at the Hartree-Fock (HF) level of theory. Although it is well- known that approximate $I(\mathbf{r})$ computed at the HF level do not possess the correct electron coalescence cusp at the origin [18], it has been recently shown that the main topological features are already manifested in approximate densities from HF calculations [20, 21]. Atomic calculations were done with the program Atomic-86 [23], which generates spherically averaged electronic wavefunctions, using a 6-311G basis set. Molecular calculations were performed by means of the Gamess-96 package [24], using a 6-31G** basis set for the isoelectronic series of molecules and a 6-311++G** basis set for the chemical reactivity study. The restricted HF method was used for all closed-shell systems and the unrestricted HF method for the only open-shell system, $H_2/H^\bullet$.

Calculations of $I(\mathbf{r})$ and $E(\mathbf{R})$, as well as their respective Laplacians, were performed numerically following the algorithm recently described by Cioslowski and Liu [19]. For spherical systems it is sufficient to compute $I(\mathbf{r})$ and $E(\mathbf{R})$ along an axis starting at the nuclear position. Accordingly, Y_{AB} and X_{AB} for atomic systems were numerically evaluated as

$$Y_{AB} \approx 4\pi \sum I_A(r) I_B(r) r^2 \Delta r \ , \quad (7)$$

$$X_{AB} \approx 4\pi \sum E_A(r) E_B(r) r^2 \Delta r \ , \quad (8)$$

using a 15 a.u. radius and a 0.01 a.u. grid spacing (Δr), with an integral neglect threshold of 10^{-8}. For linear systems, cylindrical $I(\mathbf{r})$ and $E(\mathbf{R})$ distributions can be generated by rotating a planar grid around the internuclear axis. Therefore, Y_{AB} and X_{AB} for linear molecular systems were numerically computed as

$$Y_{AB} \approx 2\pi \sum I_A(x,z) I_B(x,z) x \Delta x \Delta z \ , \quad (9)$$

$$X_{AB} \approx 2\pi \sum E_A(x,z) E_B(x,z) x \Delta x \Delta z \ , \quad (10)$$

where z and x are the rotation axis (the axis along which the molecular system is aligned) and an axis perpendicular to it, respectively. In this case, the coordinates of the rectangular grid defined for $I(\mathbf{r})$ and $E(\mathbf{R})$ distributions were extended 10 and 5 a.u. out of the outermost atoms, respectively, using a grid spacing of 0.02 and 0.01 a.u., respectively, with an integral neglect threshold of 10^{-5}. Values selected for the extension and spacing of the grids and for the integral neglect threshold were taken from a previous systematic study of these parameters on various atomic and molecular systems [25].

Following the original definition of the Carbó similarity index (C_{AB}) using first-order quantum similarity measures [1], a Carbó similarity index using second-order quantum similarity measures ($C_{AB}^{(2)}$) can be generally defined as [10]

$$C_{AB}^{(2)} = \frac{Z_{AB}^{(2)}}{(Z_{AA}^{(2)} Z_{BB}^{(2)})^{1/2}} \ . \quad (11)$$

In this particular work of the use of $I(\mathbf{r})$ and $E(\mathbf{R})$ instead of $\Gamma(\mathbf{r}_1, \mathbf{r}_2)$ implies that second-order quantum similarity indices will be evaluated using intracule (Y) and extracule (X) quantum similarity measures, which will replace the $Z^{(2)}$ general notation in Eq. (11).

3 Results and discussion

Three examples are selected to illustrate the use of second-order quantum similarity measures for quantitative analysis of electron-pair density distributions. At a first level, quantum self-similarity measures obtained for a series of atoms will be presented. Then, the discussion will be extended to the evaluation and optimization of quantum similarity measures and indices when comparing a series of isoelectronic molecules. Finally, a study of the electron-pair density reorganization in a series of model hydrogen-transfer reactions will be performed.

3.1 Atomic systems

Evaluation of $\rho(\mathbf{r})$, $I(\mathbf{r})$ and $E(\mathbf{R})$ was carried out for the series of He, Li, Be, and Ne atoms. Calculation of the respective Laplacians ($\nabla^2\rho(\mathbf{r})$, $\nabla^2 I(\mathbf{r})$, and $\nabla^2 E(\mathbf{R})$) revealed the typical pairs of spherical regions of alternating density concentration (negative values) and depletion (positive values) which reflect the shell structure of atoms [14, 26]. Thus, for example, the shell structures revealed by $\nabla^2\rho(\mathbf{r})$ and $\nabla^2 I(\mathbf{r})$ for the Neon atom can be visually compared in Fig. 1. Although it has been previously stated that $\nabla^2\rho(\mathbf{r})$ and $\nabla^2 I(\mathbf{r})$ exhibit comparable shell structures because similar values for the corresponding radii of minima are found [14], their conceptual interpretation is essentially different [21, 25].

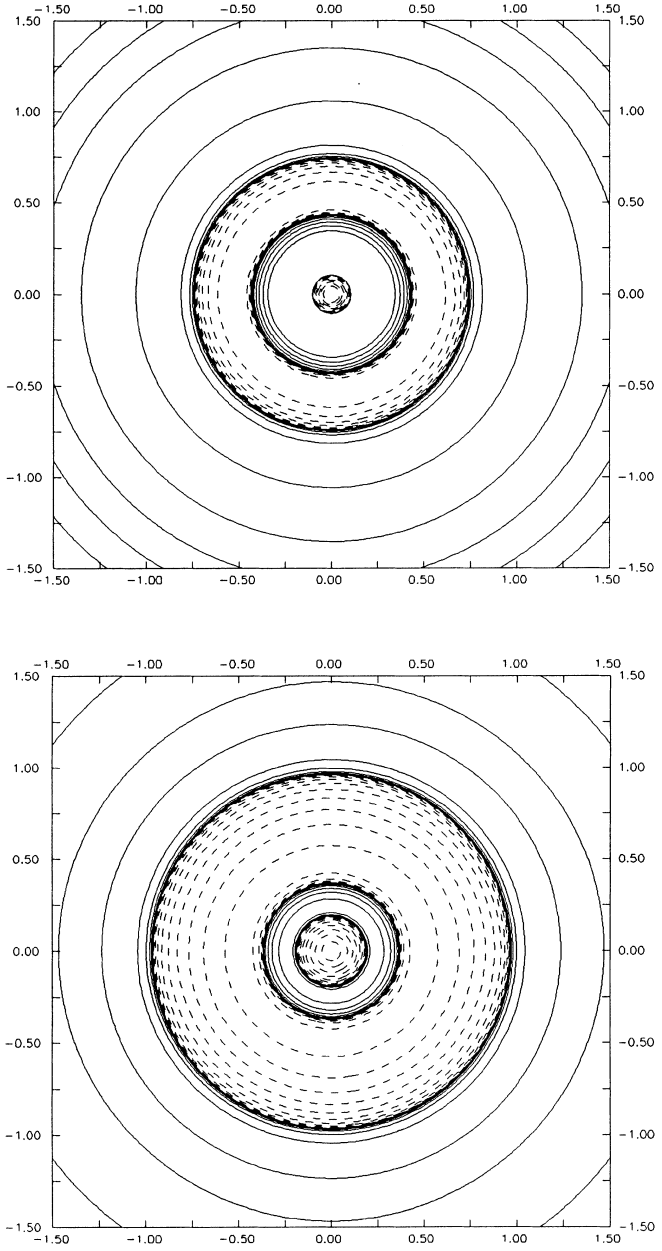

Fig. 1. Laplacian of the one-electron density (top) and Laplacian of the intracule density (bottom) for the Ne atom. Positive values are depicted in *solid lines* and negative values in *dashed lines*

A quantitative study on the nature of the shell structure of atoms, as defined by $\nabla^2\rho(\mathbf{r})$, $\nabla^2 I(\mathbf{r})$ and $\nabla^2 E(\mathbf{R})$, in terms of the number of electrons (n) and Z_{AA} (for $\rho(r)$) and the number of electron pairs ($N = (n^2 - n)/2$) and Y_{AA} (for $I(\mathbf{r})$) or X_{AA} (for $E(\mathbf{R})$) was performed. Results for the series of He, Li, Be, and Ne atoms are presented in Table 1. Among the atoms, the He atom represents the simplest case. It has 2 electrons, 1 electron pair, in a single shell ($1s^2$). The electron probability in $\rho(\mathbf{r})$ and the electron-pair probability in both $I(\mathbf{r})$ and $E(\mathbf{R})$ are found to be exactly (within four decimal figures) 2 and 1, respectively. This result serves also to validate the numerical integration scheme used in this work [25].

The Li atom has 3 electrons, 2 in the *core* shell and 1 in the *valence* shell ($1s^2 2s^1$). This electron distribution gives rise to 3 electron pairs: 1 *core* intra-shell and 2 *core-valence* inter-shell. The values of these *formal* probabilities agree well with the values found by numerical integration of the corresponding densities within the spatial domains of the shells, as defined by the respective Laplacians: electron probabilities for the two shells in $\rho(\mathbf{r})$ are 2.13 and 0.87, whereas electron-pair probabilities for the two shells in both $I(\mathbf{r})$ and $E(\mathbf{R})$ are 1.28 and 1.72.

With respect to the Li atom, the Be atom contains an additional electron occupying its *valence* shell ($1s^2 2s^2$). As a result, 6 electron pairs are now possible within this *formal* electron distribution: 1 *core* intra-shell, 4 *core-valence* inter-shell, and 1 *valence* intra-shell. Accordingly, electron probabilities for the two shells in $\rho(\mathbf{r})$ are 2.20 and 1.80, and electron-pair probabilities for the two shells in both $I(\mathbf{r})$ and $E(\mathbf{R})$ are 1.47 and 4.53, in qualitative agreement with the expected *formal* probabilities.

In the case of the Ne atom ($1s^2 2s^2 p^6$), the 2 *core* electrons and the 8 *valence* electrons can be combined in 45 electron pairs: 1 *core* intra-shell, 16 *core-valence* inter-shell, and 28 *valence* intra-shell. The electron probabilities for the two shells in $\rho(\mathbf{r})$, 2.91 and 7.09, show a large deviation from the expected *formal* probabilities. Improvement of the basis set did not provide a better electronic description of the shell. This result could be attributed to the fact that shells defined by $\nabla^2\rho(\mathbf{r})$ are slightly more extended than shells defined by the radial density function [26]. Interestingly, electron-pair probabilities of the two shells in $I(\mathbf{r})$ and $E(\mathbf{R})$ now seem to be more dependent on the contraction of the electron-pair density: while probabilities of 2.45 and 42.55 are obtained in $I(\mathbf{r})$, values of 2.96 and 42.04 are found in $E(\mathbf{R})$. Thus, the inner electron-pair shell becomes more populated in $E(\mathbf{R})$ whereas, consequently, the outer electron-pair shell appears less populated in $E(\mathbf{R})$. This effect was not noticed previously in the electron-pair shell structures of Li and Be, where practically identical electron-pair probabilities were obtained in $I(\mathbf{r})$ and $E(\mathbf{R})$. The reason for this trend can be explained by considering the definition of intracule and extracule coordinates: as the number of electrons in the *valence* shell increases, more *valence* intra-shell electron-pair interac-

Table 1. Atomic-shell quantum self-similarity measures (in a.u.) as computed from one-electron (z), intracule (y), and extracule (x) densities. n and N stand for the one-electron and electron-pair probabilities for each atomic shell, respectively. Also included are the corresponding total atomic quantum self-similarity measures (Z, Y, and X in boldface)

Atoms	n_1	z_1	n_2	z_2	Z_{AA}
He	2.0000	0.7618			**0.7618**
Li	2.1277	3.1373	0.8723	0.0012	**3.1386**
Be	2.1986	8.3750	1.8014	0.0173	**8.3923**
Ne	2.9115	163.9633	7.0884	6.1405	**170.1036**
	N_1	y_1	N_2	y_2	Y_{AA}
He	1.0000	0.0449			**0.0449**
Li	1.2807	0.2004	1.7192	0.0046	**0.2050**
Be	1.4706	0.5987	4.5294	0.0840	**0.6827**
Ne	2.4520	33.3623	42.5479	101.0167	**134.3790**
	N_1	x_1	N_2	x_2	X_{AA}
He	1.0000	0.3595			**0.3595**
Li	1.2801	1.6033	1.7190	0.0366	**1.6399**
Be	1.4688	4.7889	4.5312	0.6728	**5.4617**
Ne	2.9604	364.4124	42.0396	897.9395	**1262.3519**

tions with a probability of finding their center of mass in the vicinities of the origin will also furnish the inner electron-pair shell in $E(\mathbf{R})$, thus making the inner-shell electron-pair probability larger than it would be expected from the number of *core* electrons only.

From Table 1 it can also be seen that values of Z_{AA}, Y_{AA} and X_{AA} along this series of atoms follow a similar trend. It was recently shown that the value of Z_{AA} increases with the number of electrons in the atomic system [5]. Since the larger the number of electrons, the larger the number of electron pairs, Y_{AA} and X_{AA} also increase in the same direction. Furthermore, interesting issues emerge from examination of the atomic-shell quantum self-similarity measures. On the one hand, it can be observed that values of z_1 in Li, Be, and Ne represent 99.96%, 99.79%, and 96.39% of the Z_{AA} value, respectively, thus reflecting the well-known fact that the one-electron density of quantum systems is strongly dominated by *core* electrons. On the other hand, values of y_1 in Li, Be, and Ne suffer a much larger variation as they represent 97.76%, 87.70%, and 24.83% of the Y_{AA} value, respectively, and similar decay is obtained for x_1 values, representing 97.77%, 87.68%, and 28.87% of the X_{AA} value, respectively. This indicates that $I(\mathbf{r})$ and $E(\mathbf{R})$ are much smoother than $\rho(\mathbf{r})$ and, consequently, more sensitive to *valence* electrons. This finding suggests the use of Y_{AA} and X_{AA} as alternative quantitative measures for analyzing electron density reorganizations in chemical reactivity studies (vide infra).

3.2 Molecular systems

In this section, the series of C_2H_2, HCN, CNH, CO, and N_2 linear isoelectronic molecules will be considered, and $\rho(\mathbf{r})$, $I(\mathbf{r})$, and $E(\mathbf{R})$ distributions calculated for each molecule. In contrast with the ease of interpretation of $\rho(\mathbf{r})$, a correct interpretation of the topology of $I(\mathbf{r})$ and $E(\mathbf{R})$ in molecules requires a much more careful examination [20, 21]. For the sake of comparison, the profiles of $\rho(\mathbf{r})$ and $E(\mathbf{R})$ along the internuclear axis in N_2 and CO are presented in Fig. 2. For N_2, two symmetric attractors at nuclei positions are observed in the $\rho(\mathbf{r})$ profile, whereas three attractors appear in the corresponding $E(\mathbf{R})$ profile. In this latter profile, the stronger attractor at the origin can be associated with electron-pair internuclear interactions while the other two attractors located at nuclei positions arise from electron-pair intra-nuclear interactions [20, 21]. Similar interpretations can be derived for the CO profiles.

Because of the existence of several attractors in the various molecular density profiles, the optimal comparison between two molecules will be achieved by maximizing the quantum similarity measure (or index) through optimization of their relative position. As the molecules considered in this work are linear, the relative position between two molecules will be given by their displacement along the internuclear axis, $\mathbf{d} = \mathbf{c}_A - \mathbf{c}_B$, where $\mathbf{c}_A$ and $\mathbf{c}_B$ are the coordinates of the centers of mass of molecules A and B, respectively. Interestingly, it must be emphasized here that, since $I(\mathbf{r})$ is invariant to translations of the nuclear framework, if linear molecules are previously aligned along the same axis, no optimization procedure is required to maximize Y_{AB}.

The variations of C_{AB} and $C_{AB}^{(2)}$ depending on the relative position of two molecules ($\mathbf{d}$) define the $C_{AB}(\mathbf{d})$ and $C_{AB}^{(2)}(\mathbf{d})$ similarity-index functions, respectively. As it has been stated that Y_{AB} is not dependent on relative translations of the molecules and only linear molecules are considered in this work, $C_{AB}^{(2)}(\mathbf{d})$ functions will be evaluated solely from extracule quantum similarity measures. $C_{AB}(\mathbf{d})$ and $C_{AB}^{(2)}(\mathbf{d})$ functions for the comparison between N_2 and CO are depicted in Fig. 3. For the sake of clarity, a scheme of the superposition of the two molecules associated with the different attractors found in the topologies of $C_{AB}(\mathbf{d})$ and/or $C_{AB}^{(2)}(\mathbf{d})$ has been added. As $\rho(\mathbf{r})$ and $E(\mathbf{R})$ represent different electronic features of the molecule (Fig. 2), distinct topologies are observed. In this particular case, the global maxima in $C_{AB}(\mathbf{d})$ and $C_{AB}^{(2)}(\mathbf{d})$ are achieved at the same relative position between the two molecules. In $C_{AB}(\mathbf{d})$ the global maximum corresponds to the overlap between the pairs of two attractors in $\rho(\mathbf{r})$ located at the nuclei positions, whereas in $C_{AB}^{(2)}(\mathbf{d})$ it is associated with the overlap between the pairs of three attractors in $E(\mathbf{R})$ commented on above (see Fig. 2). The position of this global maxima is not found exactly at $\mathbf{d} = 0.00$ a.u. but at $\mathbf{d} = 0.01$ a.u. due to the presence of a stronger attractor at the oxygen

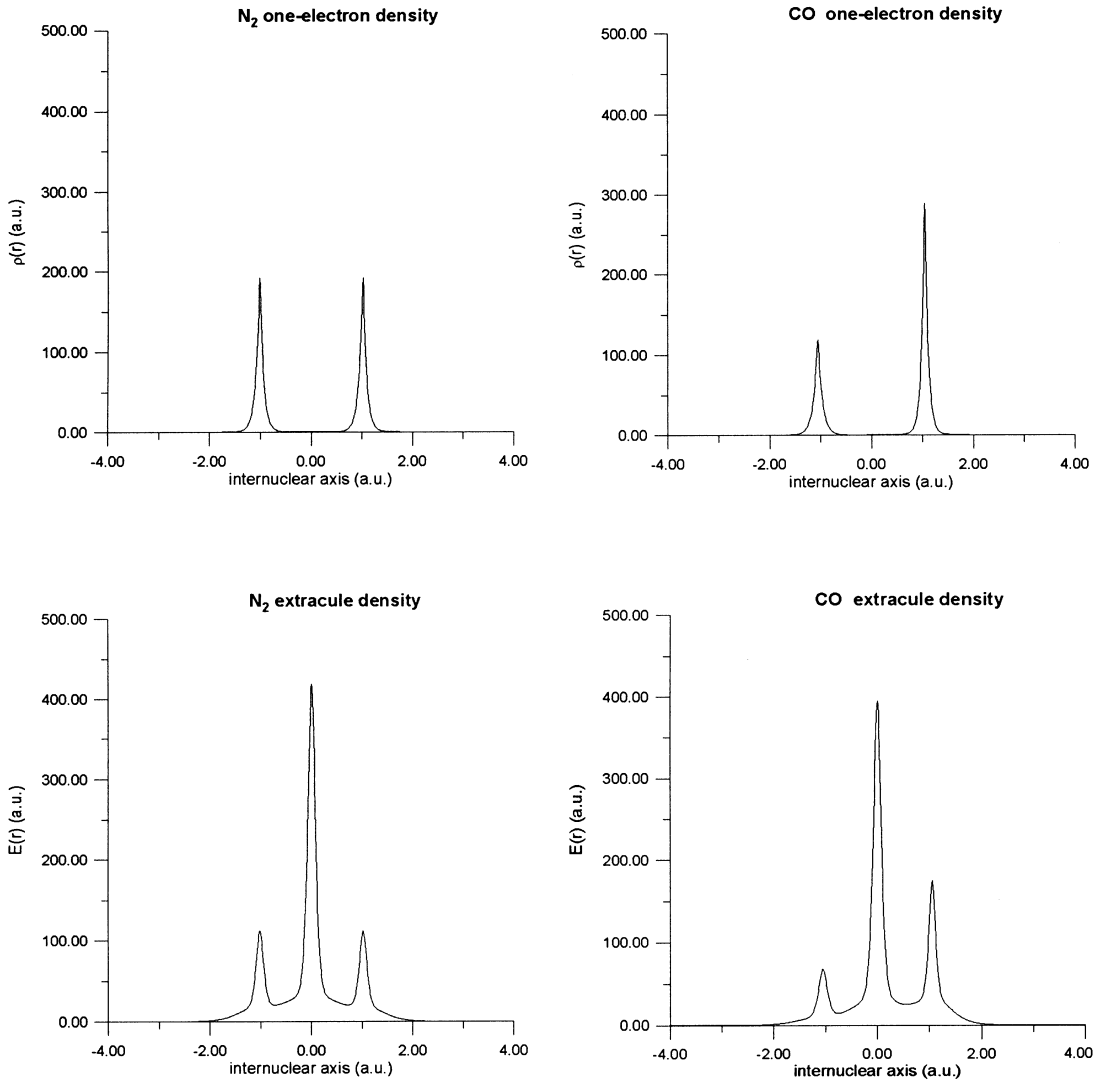

Fig. 2. One-electron densities (*top*) and extracule densities (*bottom*) for the N_2 and CO molecules

position in $\rho(\mathbf{r})$ and $E(\mathbf{R})$ for CO, which induces some assymmetry in the similarity-index functions.

Besides the global maxima, two additional local maxima are located in the topology of $C_{AB}(\mathbf{d})$ (at $\mathbf{d} = -2.06$ a.u. and $\mathbf{d} = 2.06$ a.u.) and $C^{(2)}_{AB}(\mathbf{d})$ (at $\mathbf{d} = -0.98$ a.u. and $\mathbf{d} = 1.01$ a.u.). As can be observed, in comparison with local maxima in $C_{AB}(\mathbf{d})$, local maxima in $C^{(2)}_{AB}(\mathbf{d})$ are found at shorter relative positions due to the presence of the attractors at the origin in $E(\mathbf{R})$ distributions, which overlap with each one of the attractors of the other molecule located at nuclei positions. Finally, small shoulders appear in the $C^{(2)}_{AB}(\mathbf{d})$ profile at those relative positions of the molecules where $C_{AB}(\mathbf{d})$ has the two local maxima, which are attributed to overlaps between attractors located at the outermost nuclei positions.

Table 2 shows the optimized quantum similarity measures and indices for all pair-wise comparisons between the molecules in the set. The use of an isoelectronic series of molecules was found to be an interesting limit case because, since all molecules have the same number of electrons, electronic differences between them will come from local concentrations of density [5]. Then, for example, the smaller and the larger Z_{AA}, Y_{AA} and X_{AA} values obtained among all molecules in the set correspond to C_2H_2 and CO, respectively. This reflects the fact that C_2H_2 and CO have the most depleted and the most concentrated $\rho(\mathbf{r})$, $I(\mathbf{r})$, and $E(\mathbf{R})$ distributions, respectively. In contrast, closer Z_{AA}, Y_{AA} and X_{AA} values are obtained for HCN and CNH, which are in agreement with the fact that their density distributions differ only in the internal electronic reorganization caused by the presence of a hydrogen atom being attached to carbon, in HCN, or to nitrogen, in CNH. However, a closer inspection of these values reveals that, while Z_{AA} values indicate that $\rho(\mathbf{R})$ is slightly more concentrated in HCN (83.9078) than in CNH (83.8761), Y_{AA} and X_{AA} values show the opposite trend, both $I(\mathbf{r})$ and $E(\mathbf{R})$ being more depleted in HCN (110.6071 and 1092.7411, respectively) than in CNH (110.6675 and 1096.9081, respectively).

On the other hand, values of similarity indices reflect that this series of isoelectronic molecules is globally

more similar when molecular comparisons are performed from electron-pair densities than from the one-electron density. A closer examination of similarity indices shows that when molecules are compared using $\rho(\mathbf{r})$, the pairs of less similar molecules are $\{C_2H_2, N_2\}$, $\{C_2H_2, CO\}$, and $\{CNH, N_2\}$ with similarity indices of 0.7873, 0.8699, and 0.8728, respectively. However, when the same pairs of molecules are compared using $I(\mathbf{r})$, the similarity indices obtained are 0.9376, 0.9550, and 0.9713, and when using $E(\mathbf{R})$, similarity indices of 0.9753, 0.9634, and 0.9786 are found, respectively. In contrast, the most similar pairs of molecules according to $\rho(\mathbf{r})$ are {HCN, CNH} (0.9898) and {HCN,CO} (0.9836). The most similar pair of molecules from $I(\mathbf{r})$ is also {HCN,CNH} (0.9973), followed by the pairs $\{CO,N_2\}$ (0.9919) and {HCN,CO} (0.9903). However, when similarity indices are computed from $E(\mathbf{R})$, {HCN, CNH} is the fourth most similar pair (0.9893), behind the pairs $\{C_2H_2, HCN\}$ (0.9919), {CNH,CO} (0.9918), and $\{HCN,N_2\}$ (0.9913).

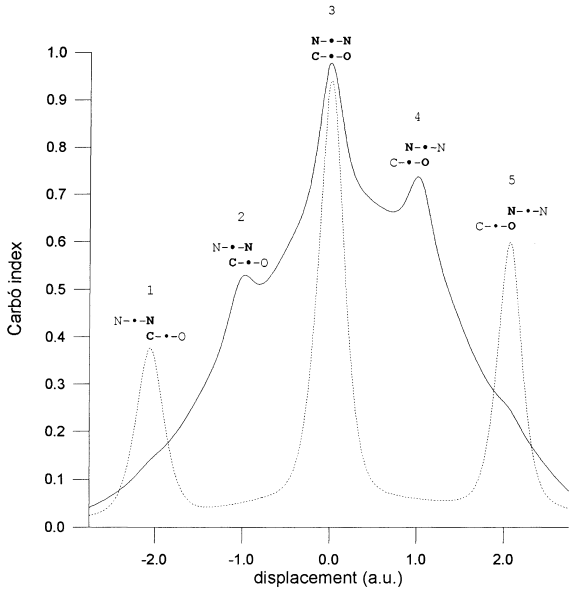

Fig. 3. Variation of C_{AB} (*dashed line*) and $C_{AB}^{(2)}$ (using extracule densities, *solid line*) depending on the superimposition of the N_2 and CO molecules. Molecular superimposition schemes are on top of each local maximum. *Dots* indicate internuclear centers. Matching features are indicated in bold

The collection of results exposed above clearly reveal that the topology of a similarity-index function depends on the particular electron-density description of molecules used to evaluate the similarity index. For instance, in cases where the differences between the topologies of $\rho(\mathbf{r})$ and $E(\mathbf{R})$ in the two molecules are accentuated, it has been observed that even the global maxima on $C_{AB}(\mathbf{d})$ and $C_{AB}^{(2)}(\mathbf{d})$ can be achieved at different relative positions [25]. This only supports the well-known fact that molecular similarity cannot be unequivocally defined, but depends on the particular molecular representation used for its evaluation.

3.3 Application to chemical reactivity

In order to illustrate the potential applicability of first-order and second-order quantum similarity measures and indices for quantitatively analyzing one-electron and electron-pair reorganizations in chemical reactivity, a comparative study on a series of model hydrogen-transfer reactions is presented. The systems H_2/H^+, $H_2/H^\bullet$ and H_2/H^- were taken as the simplest models where hydride (H^-), hydrogen ($H^\bullet$) and proton (H^+) transfers occur. The three processes considered are illustrated in Eqs. (12)–(14).

$$H_2 + H^+ \rightarrow [H_l - H_t - H_r]^+ \rightarrow H^+ + H_2, \tag{12}$$

$$H_2 + H^\bullet \rightarrow [H_l - H_t - H_r]^\bullet \rightarrow H^\bullet + H_2, \tag{13}$$

$$H_2 + H^- \rightarrow [H_l - H_t - H_r]^- \rightarrow H^- + H_2 \ . \tag{14}$$

Table 2. Quantum similarity measures (plain values below the diagonal, in a.u.) and indices (values in italics above the diagonal) for the best pair-wise molecular alignments in the C_2H_2, HCN, CNH, CO, and N_2 isoelectronic series as computed from one-electron, intracule, and extracule densities. Values in boldface on the diagonal are the corresponding quantum self-similarity measures

One-electron density					
	C_2H_2	HCN	CNH	CO	N_2
C_2H_2	**63.1901**	*0.9341*	*0.9681*	*0.8699*	*0.7873*
HCN	68.0174	**83.9078**	*0.9898*	*0.9836*	*0.9247*
CNH	70.4763	83.0377	**83.8761**	*0.9604*	*0.8728*
CO	73.3567	95.5820	93.3107	**112.5459**	*0.9410*
N_2	64.0142	86.6401	81.7599	102.1060	**104.6179**
Intracule density					
	C_2H_2	HCN	CNH	CO	N_2
C_2H_2	**84.9719**	*0.9830*	*0.9887*	*0.9550*	*0.9376*
HCN	95.2967	**110.6071**	*0.9973*	*0.9903*	*0.9816*
CNH	95.8785	110.3395	**110.6675**	*0.9859*	*0.9713*
CO	106.9105	126.4835	125.9488	**147.4734**	*0.9919*
N_2	103.6836	123.8371	122.5762	144.4941	**143.9068**
Extracule density					
	C_2H_2	HCN	CNH	CO	N_2
C_2H_2	**833.2894**	*0.9919*	*0.9839*	*0.9634*	*0.9753*
HCN	946.5369	**1092.7411**	*0.9893*	*0.9830*	*0.9913*
CNH	940.6793	1083.1603	**1096.9081**	*0.9918*	*0.9786*
CO	1065.7657	1245.2987	1258.9200	**1468.7070**	*0.9782*
N_2	1064.7219	1239.1688	1225.6732	1417.7297	**1430.1182**

The notation H_l, H_t and H_r will be used to refer to the outermost hydrogen on the left-handside originally linked to the transferring hydrogen, the transferring hydrogen, and the outermost hydrogen on the right-handside finally accepting the transferring hydrogen, respectively. For comparative purposes, in all cases the distance between the two outermost hydrogens was restricted to 3 Å. Under this constraint, the concept of "stationary point" is lost and thus, it will be referred to as the "reactant complex" at the point on the reaction coordinate where the hydrogen begins to be transferred, and as the "transition state" at the point on the reaction coordinate where the hydrogen being transferred is midway. An analogous comparative analysis of $\rho(\mathbf{r})$ distributions between the hydrogen transfers in the CH_4/CH_3^+, $CH_4/CH_3^{\bullet}$ and CH_4/CH_3^- systems was recently reported [27].

All $\rho(\mathbf{r})$, $I(\mathbf{r})$ and $E(\mathbf{R})$ distributions were evaluated at the reactant complex (RC) and transition state (TS) of the three processes considered. For the sake of comparison, the corresponding $\rho(\mathbf{r})$ and $E(\mathbf{R})$ profiles along the internuclear axis of the reactions are presented in Fig. 4, where H_l is always located at the origin of the coordinates. Focusing first our attention in the $\rho(\mathbf{r})$ profiles, it is observed that similar profiles are obtained for the RC of the $H_2/H^{\bullet}$ and H_2/H^- systems, both showing a significant one-electron density probability on H_r. In contrast, the profile obtained for the RC of the H_2/H^+ system presents an expected very low density maximum on H_r. The situation becomes clearly different when observing the $\rho(\mathbf{r})$ profiles obtained at the TS. Two symmetric maxima appear centered at H_l and H_r, and one maximum centered at H_t. This situation is a direct consequence of the symmetry of the processes.

As mentioned above, in contrast to the ease of interpretation of $\rho(\mathbf{r})$ profiles, a correct interpretation of $E(\mathbf{R})$ profiles requires more careful examination. Therefore, the topology of the $E(\mathbf{R})$ profiles at the RC will be analyzed first in detail. In the H_2/H^+ system, the $E(\mathbf{R})$ profile shows a single maximum around the H_2 mid-bond position. This reflects the fact that the two electrons of this system have a very large probability of

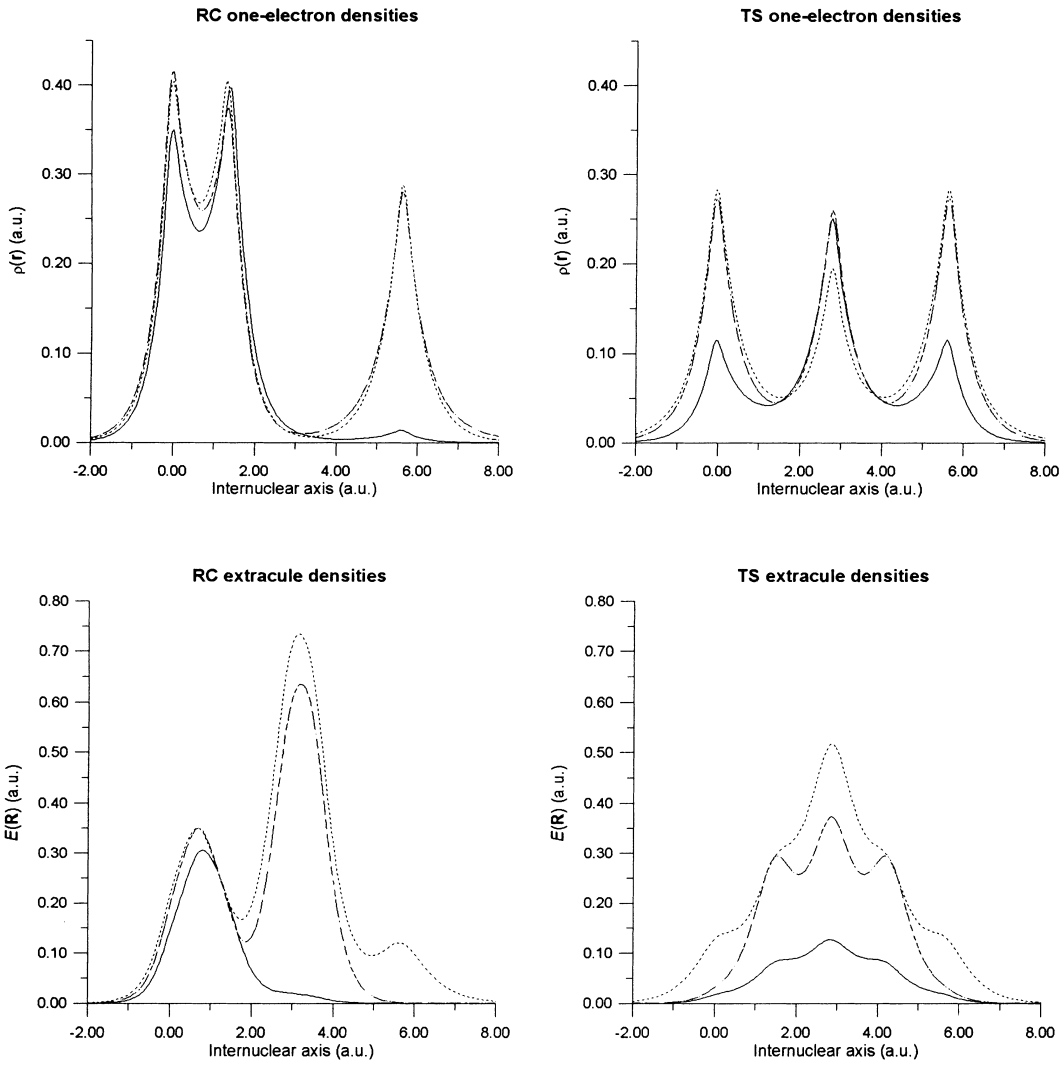

Fig. 4. One-electron densities (*top*) and extracule densities (*bottom*) at the reactant complex (*left*) and transition state (*right*) for the systems H_2/H^+ (*continuous line*), $H_2/H^{\bullet}$ (*dashed line*), and H_2/H^- (*dotted line*)

being in either one of the hydrogens of the original H_2 fragment (H_l and H_t). A small shoulder can also be observed at the average position of the centers of mass corresponding to the $\{H_l, H_r\}$ and $\{H_t, H_r\}$ interactions. This can be assigned to the non-null probability of having one electron on H_l or H_t and the other one on H_r, which is just a consequence of the above-mentioned presence of a very low maximum on H_r in the corresponding $\rho(\mathbf{r})$ profile. Interestingly, that shoulder becomes the highest maximum in the $E(\mathbf{R})$ profile of the $H_2/H^{\bullet}$ system. Following the same arguments, as the probability of finding an electron pair in the original H_2 fragment is essentially retained (it is only a bit higher), the existence of an additional electron on H_r (see the corresponding $\rho(\mathbf{r})$ profile) reinforces strongly the probability of having one electron on H_l or H_t and the other one on H_r. These two maxima are basically reproduced in the $E(\mathbf{R})$ profile of the H_2/H^- system. In addition, a third maximum is now observed on the H_r position, which is consistent with the probability of finding a pair of electrons on H_r.

The $E(\mathbf{R})$ profiles at the TS expose again a symmetry around the H_t position, consistent with the symmetry of the processes. A detailed discussion of the profile for the H_2/H^+ system will be performed and, for the sake of clarity, its interpretation will be rationalized in terms of the different electron-electron interactions [21]. Interpretation of the profiles for the $H_2/H^{\bullet}$ and H_2/H^- systems can then be derived following similar arguments. The $E(\mathbf{R})$ profile for the H_2/H^+ system has a single maximum centered at the H_t position. There are two types of electron-electron interactions that contribute to the probability of the center of mass of an electron pair being at this position, namely, the intra-atomic interaction of an electron pair on H_t (labelled as $\{H_t\}$) and the inter-atomic interaction between one electron on H_l and another one on H_r (labelled as $\{H_l, H_r\}$). To overcome the problem of having different electron-electron interactions contributing to the same region in space, a useful strategy is to complement the analysis of the $E(\mathbf{R})$ profile with that of the corresponding $I(\mathbf{r})$ profile [21]. Following this procedure, construction of the $I(\mathbf{r})$ profile allowed for separation of the contribution of $\{H_t\}$ from that of $\{H_l, H_r\}$ at different points in space (note that $\{H_l, H_r\}$ is the only type of electron-electron interaction contributing to the $H_l - H_r$ distance in the $I(\mathbf{r})$ profile) and revealed that the contribution of $\{H_t\}$ is much more important than that of $\{H_l, H_r\}$. Besides the existence of a maximum in the topology of the $E(\mathbf{R})$ profile, a pair of shoulders symmetrically placed at the $H_l - H_t$ and $H_l - H_r$ mid-bond positions are clearly observed. Accordingly, each one of these shoulders can be assigned to the probability of finding one electron on one of the outermost hydrogens (H_l or H_r) and one electron on H_t. In addition, a close inspection of this $E(\mathbf{R})$ profile reveals the presence of another pair of smooth shoulders centered at the positions of H_l and H_r, thus reflecting the probability of finding an electron pair on one of the outermost hydrogens.

Despite the fact that visual comparison between $\rho(\mathbf{r})$, or $E(\mathbf{R})$, profiles at the TS and those obtained at the corresponding RC in Fig. 4 qualitatively illustrates the one-electron, or electron-pair, density reorganization that takes place between these two points of the reaction coordinate, quantification of these density reorganizations can be assessed through the evaluation of first-order, or second-order, quantum similarity measures and indices. The results of this quantitative analysis are collected in Table 3. As a general trend, both first-order and second-order quantum self-similarity measures (boldface values in Table 3) at the RC and TS points along the different systems increase in the order $H_2/H^+ < H_2/H^{\bullet} < H_2/H^-$. This indicates a larger local concentration of both one-electron and electron-pair density distributions in the same direction. In this particular series of systems, the reason for this trend is mainly due to the fact that one electron is being added systematically from H_2/H^+ to $H_2/H^{\bullet}$ and then from $H_2/H^{\bullet}$ to H_2/H^-. For example, the $X_{TS,TS}$ values are $0.0365 < 0.3274 < 0.7271$.

Evaluation of first-order and second-order quantum similarity measures (plain values in Table 3) between the RC and the TS of each system allowed then for calculating the corresponding similarity indices (italic values in Table 3) between those points, and thus quantitatively analyzing the one-electron and electron-pair reorganization suffered along the reaction coordinate. First-order similarity indices obtained for the H_2/H^+, $H_2/H^{\bullet}$, and H_2/H^- systems are 0.5446, 0.7808 and 0.8625, respectively. This shows that the RC and TS in the H_2/H^+ system are significantly less similar than the RC and TS in the $H_2/H^{\bullet}$ system, and these are even less similar to the RC and TS in the H_2/H^- system. This result is consistent with a much larger one-electron density reorganization in the hydride-transfer process than in the proton-transfer process, with the hydrogen-transfer process lying in between.

Second-order similarity indices calculated from $E(\mathbf{R})$ distributions for the H_2/H^+, $H_2/H^{\bullet}$, and H_2/H^- systems are 0.4570, 0.8698 and 0.9497, respectively. Interestingly, comparison with the previously discussed first-order similarity indices indicates that, from the point of view of the electron-pair density reorganization, while the RC and TS in the H_2/H^+ system are clearly less similar, the RC and TS in the $H_2/H^{\bullet}$ and H_2/H^- systems become more similar. Taking the H_2/H^+ and H_2/H^- systems as the two limit cases, this result is in good agreement with the fact that, while the hydrogen nucleus being transferred in the H_2/H^+ system formally

Table 3. Quantum similarity measures (QSM) in a.u. and indices (values in italics) between the RC and TS for the three model hydrogen-transfer systems studied. Quantum self-similarity measures are given in boldface

QSM		H_2/H^+		$H_2/H^{\bullet}$		H_2/H^-	
		RC	TS	RC	TS	TC	TS
Z	RC	**0.1539**	*0.5446*	**0.2152**	*0.7808*	**0.2279**	*0.8625*
	TS	0.0538	**0.0635**	0.1274	**0.1238**	0.1568	**0.1451**
Y	RC	**0.0105**	*0.8915*	**0.0367**	*0.8512*	**0.0770**	*0.9582*
	TS	0.0062	**0.0046**	0.0280	**0.0294**	0.0707	**0.0709**
X	RC	**0.0841**	*0.4570*	**0.4743**	*0.8698*	**0.8758**	*0.9497*
	TS	0.0253	**0.0365**	0.3427	**0.3274**	0.7578	**0.7271**

carries an electron pair along the process [28, 29], no electron pair accompanies the hydrogen nucleus being transferred in the H_2/H^- system.

Finally, second-order similarity indices calculated from $I(\mathbf{r})$ distributions for the H_2/H^+, $H_2/H^\bullet$, and H_2/H^- systems are 0.8915, 0.8512 and 0.9582, respectively. Note that similarity indices found from $I(\mathbf{r})$ distributions for the $H_2/H^\bullet$ and H_2/H^- systems are consistent with those similarity indices found from $E(\mathbf{R})$ distributions. However, a significant difference is found between the second-order similarity indices for the H_2/H^+ system. This can be explained by the fact that the electron pair being transferred in the H_2/H^+ system, and thus responsible for most of the electron-pair reorganization in this system, contributes to $I(\mathbf{0})$ in the $I(\mathbf{r})$ distributions of both RC and TS points. Therefore, although for this particular process the second-order similarity index calculated from $I(\mathbf{r})$ distributions is not able to reflect the transfer of the electron pair, it is in good agreement with the fact that the two electrons are being transferred essentially as a pair [27–29].

Conclusions

The evaluation of second-order quantum similarity measures from intracule and extracule densities is revealed as an alternative type of analysis to compare quantitatively the electronic characteristics of atomic and molecular systems. In the limit case of an isoelectronic series of molecules, results show that molecules are more similar when compared by electron-pair densities than from one-electron densities. Different topologies are obtained for the similarity functions computed from one-electron and extracule densities when varying the superimposition between the two molecules and, consequently, novel molecular alignments may be exposed by the respective similarity maxima. Finally, it has been shown that second-order quantum similarity indices appear also as a suitable tool for analyzing electron-pair density reorganizations in chemical processes, thus emerging as an alternative quantitative strategy from which mechanistic aspects can be discussed. More research in this direction is underway in our laboratory.

Acknowledgements. This work has been supported by the Spanish DGICYT project no. PB95-0762. X.F. benefits from a Doctoral fellowship from the University of Girona. We also thank the Centre de Supercomputació de Catalunya (CESCA) for a generous allocation of computing time.

References

1. Carbó R, Leyda L, Arnau M (1980) Int J Quantum Chem 17:1185
2. Cioslowski J, Stefanov B, Constans P (1996) J Comput Chem 17:1352
3. Cioslowski J, Fleischmann ED (1991) J Am Chem Soc 113:64
4. Cooper DL, Allan NL (1992) J Am Chem Soc 114:4773
5. Solà M, Mestres J, Oliva JM, Duran M, Carbó R (1996) Int J Quantum Chem 58:361
6. Solà M, Mestres J, Carbó R, Duran M (1994) J Am Chem Soc 116:5909
7. Mestres J, Solà M, Carbó R, Luque FJ, Orozco M (1996) J Phys Chem 100:606
8. Oliva JM, Carbó-Dorca R, Mestres J (1996) Adv Mol Sim 1:135
9. Solà M, Mestres J, Carbó R, Duran M (1996) J Chem Phys 104:636
10. Besalú E, Carbó R, Mestres J, Solà M (1995) Top Curr Chem 173:31
11. Strnad M, Ponec R (1994) Int J Quantum Chem 49:35
12. Ponec R (1997) Int J Quantum Chem 62:171
13. Coleman AJ (1967) Int J Quantum Chem 18:457
14. Sarasola C, Domínguez L, Aguado M, Ugalde JM (1992) J Chem Phys 96:6778
15. Wang J, Tripathi AN, Smith Jr. VH (1992) J Chem Phys 97:9188
16. Wang J, Smith Jr. VH (1994) Int J Quantum Chem 49:147
17. Ugalde JM, Sarasola C (1994) Phys Rev A 49:3081
18. Cioslowski J, Stefanov B, Tang A, Umrigar C J (1995) J Chem Phys 103:6093
19. Cioslowski J, Liu G (1996) J Chem Phys 105:4151
20. Cioslowski J, Liu G (1996) J Chem Phys 105:8187
21. Fradera X, Duran M, Mestres J (1997) J Chem Phys 107:3576
22. Note that while $\Gamma(\mathbf{r}_1, \mathbf{r}_2)$ takes explicitly the position of the two electrons, $I(\mathbf{r})$ and $E(\mathbf{R})$ consider the pairs of electrons as a whole thing. Consequently, as a result of this reduction in dimensionality, some two-electron information is lost in the transformation from $\Gamma(\mathbf{r}_1, \mathbf{r}_2)$ to $I(\mathbf{r})$ and $E(\mathbf{R})$
23. Roos B, Salez C, Veillard A, Clementi E (1986) A general program for calculation of atomic SCF orbitals by the expansion method. Technical report RJ-518, IBM Research. ATOMIC 86 is an updated version by R. Carbó
24. Schmidt MW, Baldridge KK, Boatz JA, Elbert ST, Gordon MS, Jensen JH, Koseki S, Matsunaga N, Nguyen KA, Su SJ, Windus TL, Dupuis M, Montgomery JA (1993) J Comput Chem 14:1347
25. Fradera X, Duran M, Mestres J Adv Mol Sim (in press)
26. Shi Z, Boyd RJ (1988) J Chem Phys 88:4375
27. Mestres J, Duran M, Bertrán J (1996) Can J Chem 74:1253
28. Mestres J, Lledós A, Duran M, Bertrán J (1992) J Mol Struct (Theochem) 260:259
29. Mestres J, Duran M, Bertrán J (1994) Theor Chim Acta 88:325